Large seafloor rupture caused by the 1956 Amorgos tsunamigenic earthquake, Greece

Leclerc[1*] Frédérique, Sylvain Palagonia [1], Nathalie Feuillet[2], Paraskevi Nomikou[3], Danai Lampridou[3], Paul Barrière[1], Alexandre Dano[1], Eduardo Ochoa[4], Nuno Gracias[4], Javier Escartin[5]

1- Université Côte d'Azur, CNRS, Observatoire de la Côte d'Azur, IRD, Géoazur, 250 rue Albert Einstein, Sophia Antipolis 06560 Valbonne, France.
2- Université Paris Cité, Institut de Physique du Globe de Paris, CNRS, F-75005, Paris, France
3- Department of Geology and Geoenvironment, National and Kapodistrian University of Athens, Panepistimioupoli Zografou, Athens, 15784, Greece
4- Computer Vision and Robotics Institute, University of Girona, Girona, Spain
5- Laboratoire de Géologie, Ecole Normale Supérieure (CNRS UMR 8538), PSL Research University, Paris, France

** Corresponding author : leclerc@geoazur.unice.fr

Extended data figure and table

This file contains the supplementary figures S1, S2, and S3, and the supplementary tables S4 and S5.

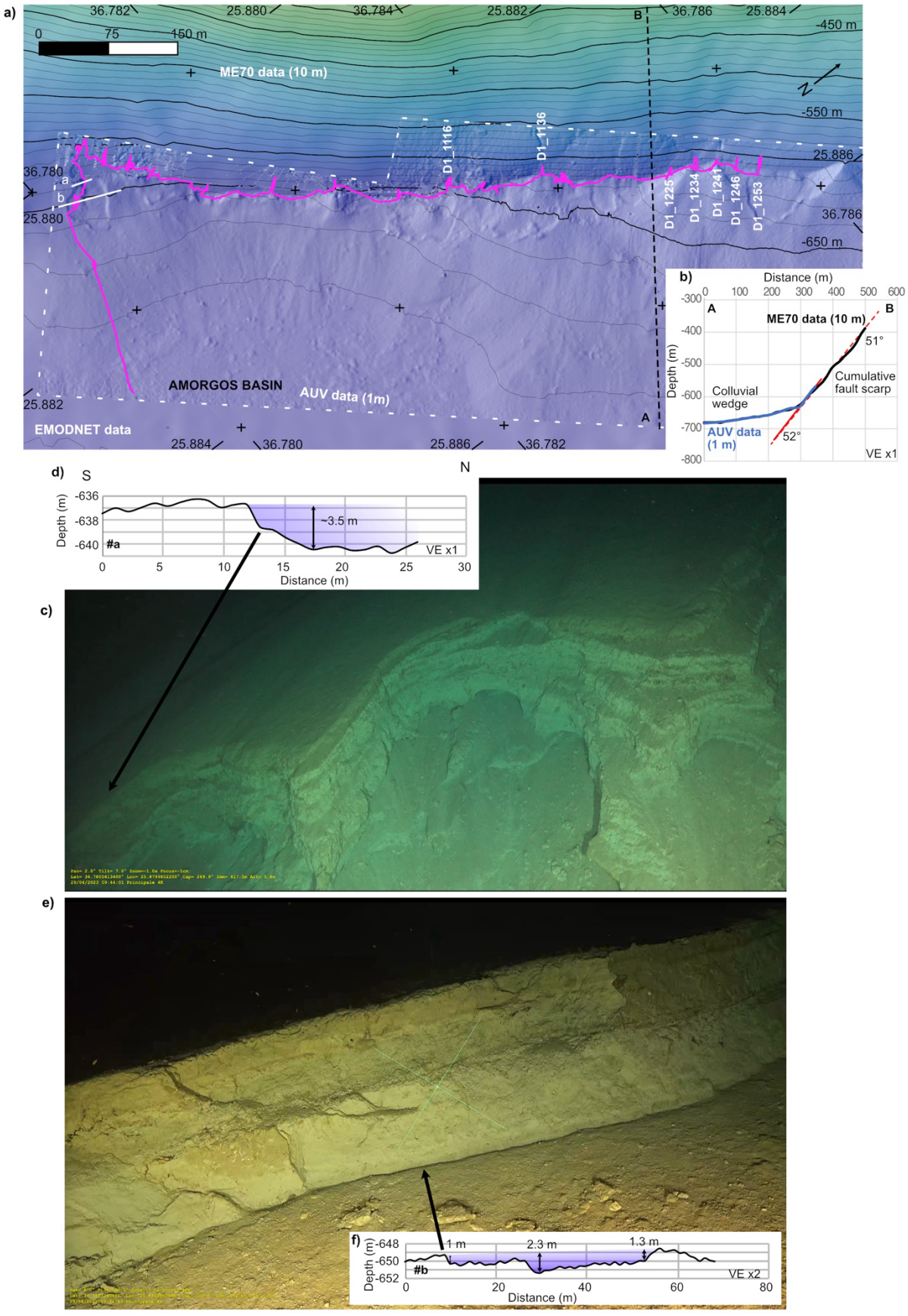
a)
36.782
25.880
36.784
25.882
B
36.786
25.884
-450 m
0
75
150 m
ME70 data (10 m)
-550 m
D1_1116
D1_1136
25.886
36.780
a
b
25.880
D1_1225
D1_1234
D1_1241
D1_1246
D1_1253
36.786
-650 m
AMORGOS BASIN
AUV data (1m)
25.882
A
EMODNET data
25.884
36.780
25.886
36.782
b)
Distance (m)
0
100
200
300
400
500
600
-300
-400
-500
-600
-700
-800
Depth (m)
A
B
ME70 data (10 m)
51°
Cumulative fault scarp
Colluvial wedge
AUV data (1 m)
52°
VE x1
d)
S
N
-636
-638
-640
Depth (m)
#a
~3.5 m
VE x1
0
5
10
15
20
25
30
Distance (m)
c)
e)
f)
-648
-650
-652
Depth (m)
1 m
2.3 m
1.3 m
#b
VE x2
0
20
40
60
80
Distance (m)

Supplementary Figure S1 – Morphology of the cumulative fault scarp and of the colluvial wedge. (a) Bathymetric map showing failure scars in the colluvial wedge. The path taken by the HROV is shown in pink, while the positions of DOMs are noted in white, and a and b mark the deepest failure scar. Bathymetric profile A-B is located in dashed black line. (b) Bathymetric profile A-B obtained with both datasets (ME70 10m resolution DEM in black and AUV 1m resolution DEM in blue) shows that here the cumulative fault scarp dips by ~51°-52° here. (c) HROV image of the deepest failure scar at position a, showing the 3.5 m high southwestern wall. The wall shows that the colluvial wedge is composed of seabed parallel strata dipping gently toward the Amorgos basin. (d) Cross-section profile along the white profile a, shows that there the depression is ~3.5 m deep. (e) The same wall downstream at position b (white line), with a height of 1 m visible on the cross-section (f).

Supplementary Figure S2: The geometry of the scarp and colluvial wedge are visible in the 1m DEM (a). (b) Seventeen topographic profiles located on (a), with no vertical exaggeration, allow measuring the fault scarp dip and the colluvial wedge slope in the vicinity of the scarp. The former varies between 45 and 59° (profile #14 shows an 80°-dipping fault plane but there the bathymetric data are not complete and this might be due to an artefact). The slope of the colluvial wedge varies from 8° to 30°.

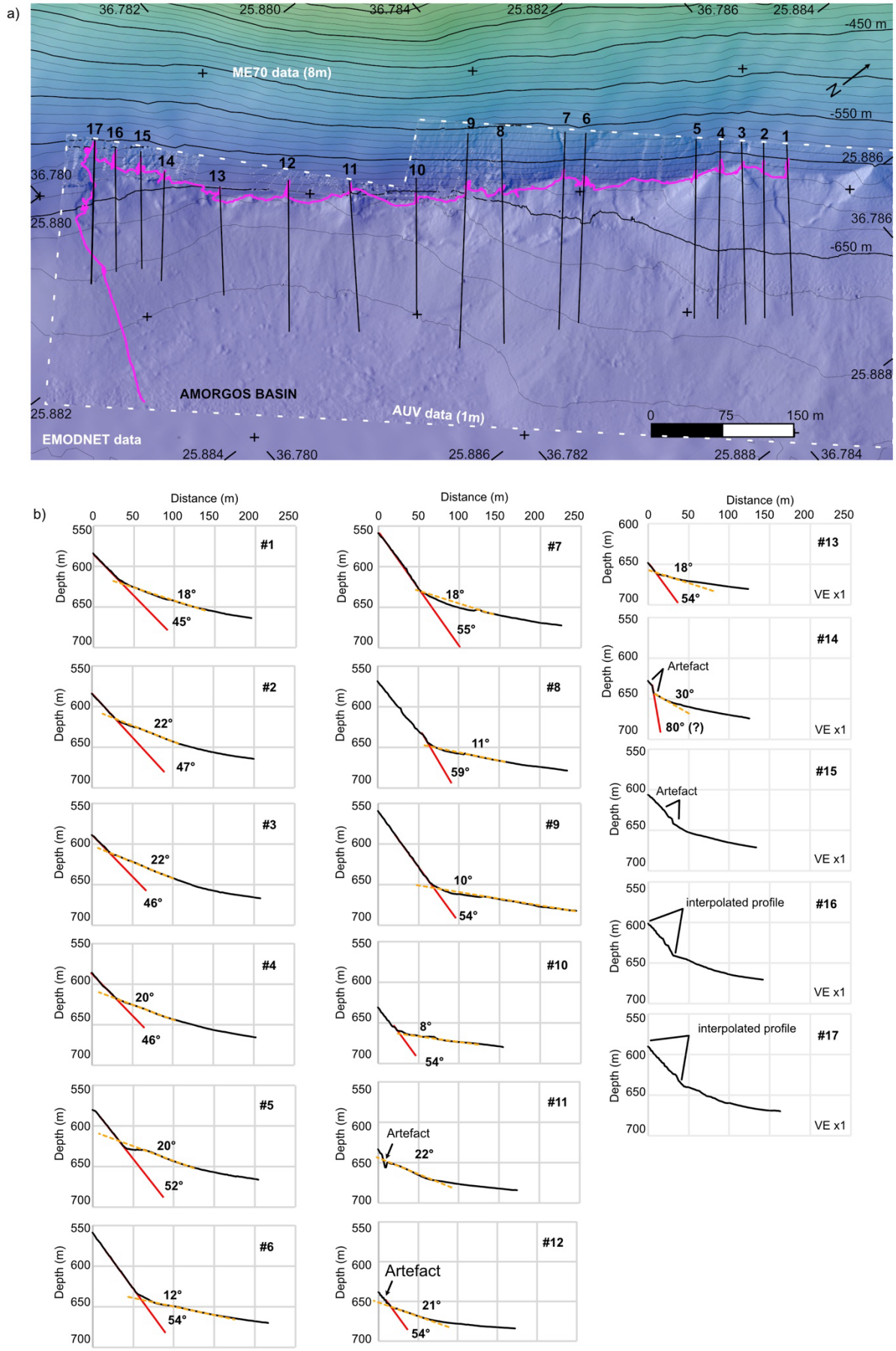
a)
36.782
25.880
36.784
25.882
36.786
25.884
-450 m
ME70 data (8m)
-550 m
17 16 15 14 13 12 11 10 9 8 7 6 5 4 3 2 1
25.886
36.780
25.880
36.786
-650 m
25.888
AMORGOS BASIN
25.882
AUV data (1m)
0 75 150 m
EMODNET data
25.884
36.780
25.886
36.782
25.888
36.784
b)
Distance (m)
Depth (m)
#1
18°
45°
#2
22°
47°
#3
22°
46°
#4
20°
46°
#5
20°
52°
#6
12°
54°
#7
18°
55°
#8
11°
59°
#9
10°
54°
#10
8°
54°
#11
Artefact
22°
#12
Artefact
21°
54°
#13
18°
54°
VE x1
#14
Artefact
30°
80° (?)
VE x1
#15
Artefact
VE x1
#16
interpolated profile
VE x1
#17
interpolated profile
VE x1

Supplementary Figure S3 – **Digital Outcrops models of the Amorgos fault, calculated with Matisse 3D (v. 1.4).** For each of the seven vertical transects, the models are presented on the upper-left panel, interpreted on the upper right panel. Located on Figure S1a. The DOMs are numbered by their acquisition time (Dive): D1_HH: MM.

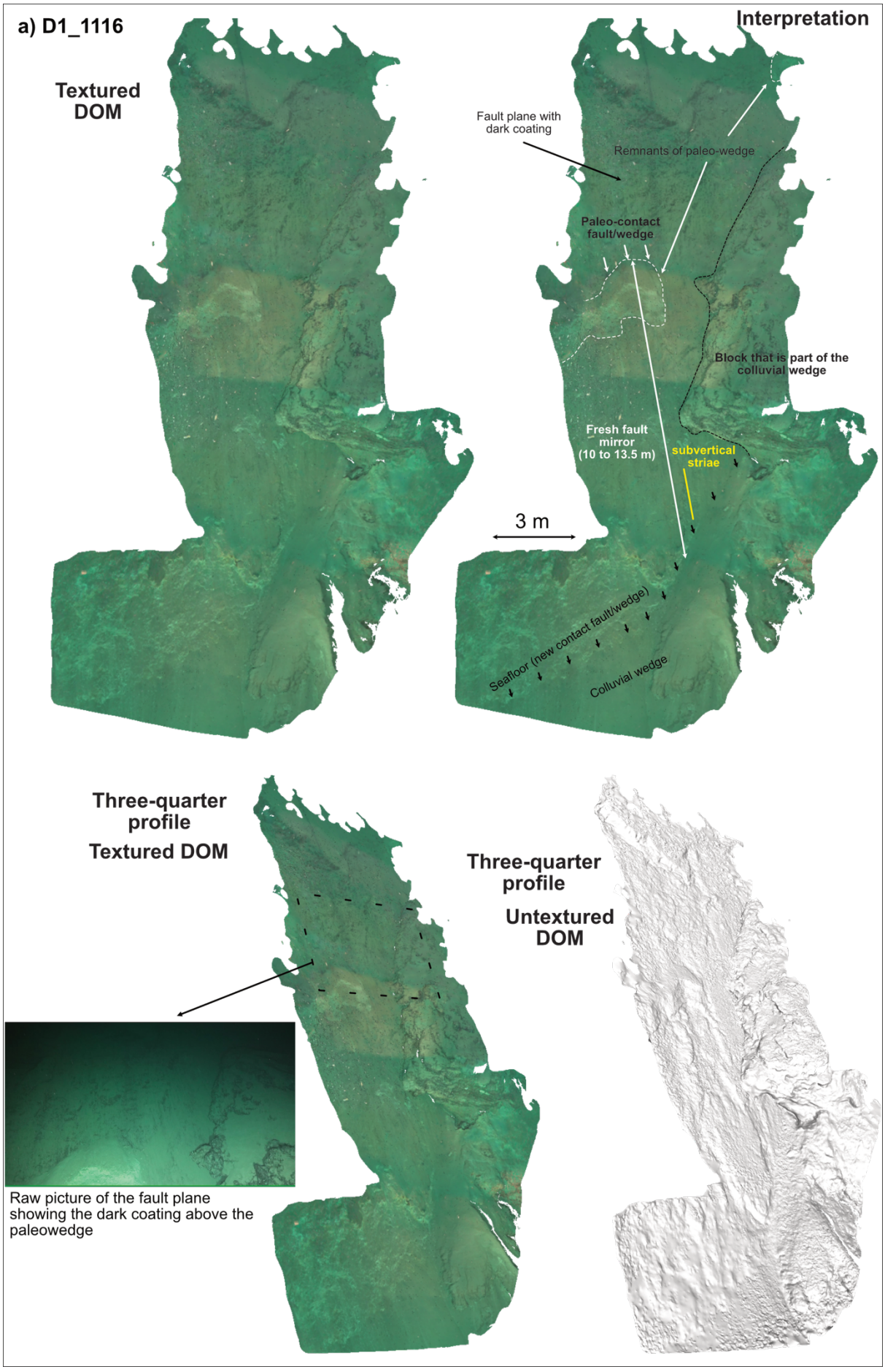
a) D1_1116
Textured DOM
Interpretation
Fault plane with dark coating
Remnants of paleo-wedge
Paleo-contact fault/wedge
Block that is part of the colluvial wedge
Fresh fault mirror (10 to 13.5 m)
subvertical striae
3 m
Seafloor (new contact fault/wedge)
Colluvial wedge
Three-quarter profile
Textured DOM
Three-quarter profile
Untextured DOM
Raw picture of the fault plane showing the dark coating above the paleowedge

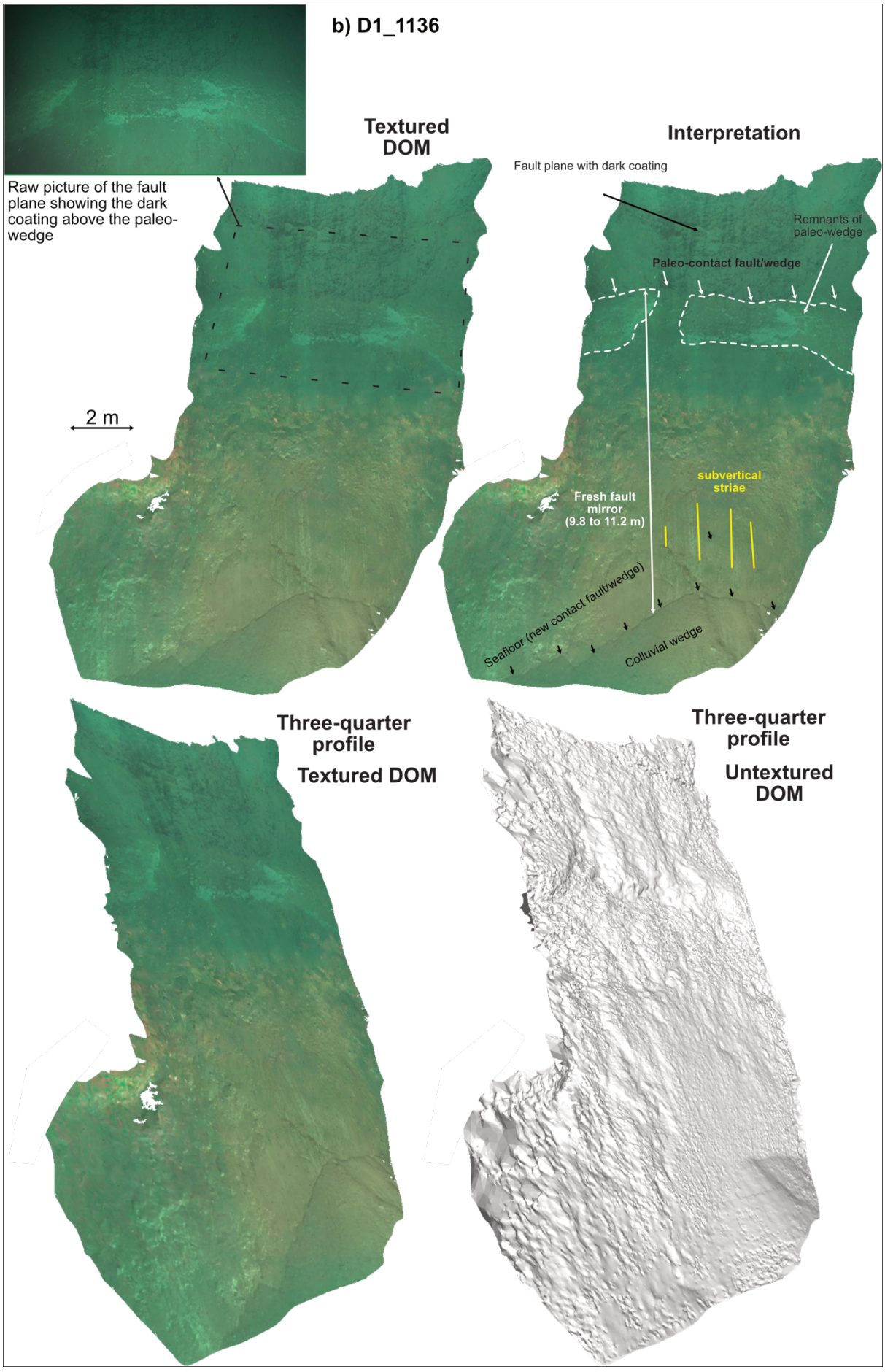
b) D1_1136
Raw picture of the fault plane showing the dark coating above the paleo-wedge
Textured DOM
Interpretation
Fault plane with dark coating
Remnants of paleo-wedge
Paleo-contact fault/wedge
2 m
Fresh fault mirror (9.8 to 11.2 m)
subvertical striae
Seafloor (new contact fault/wedge)
Colluvial wedge
Three-quarter profile
Textured DOM
Three-quarter profile
Untextured DOM

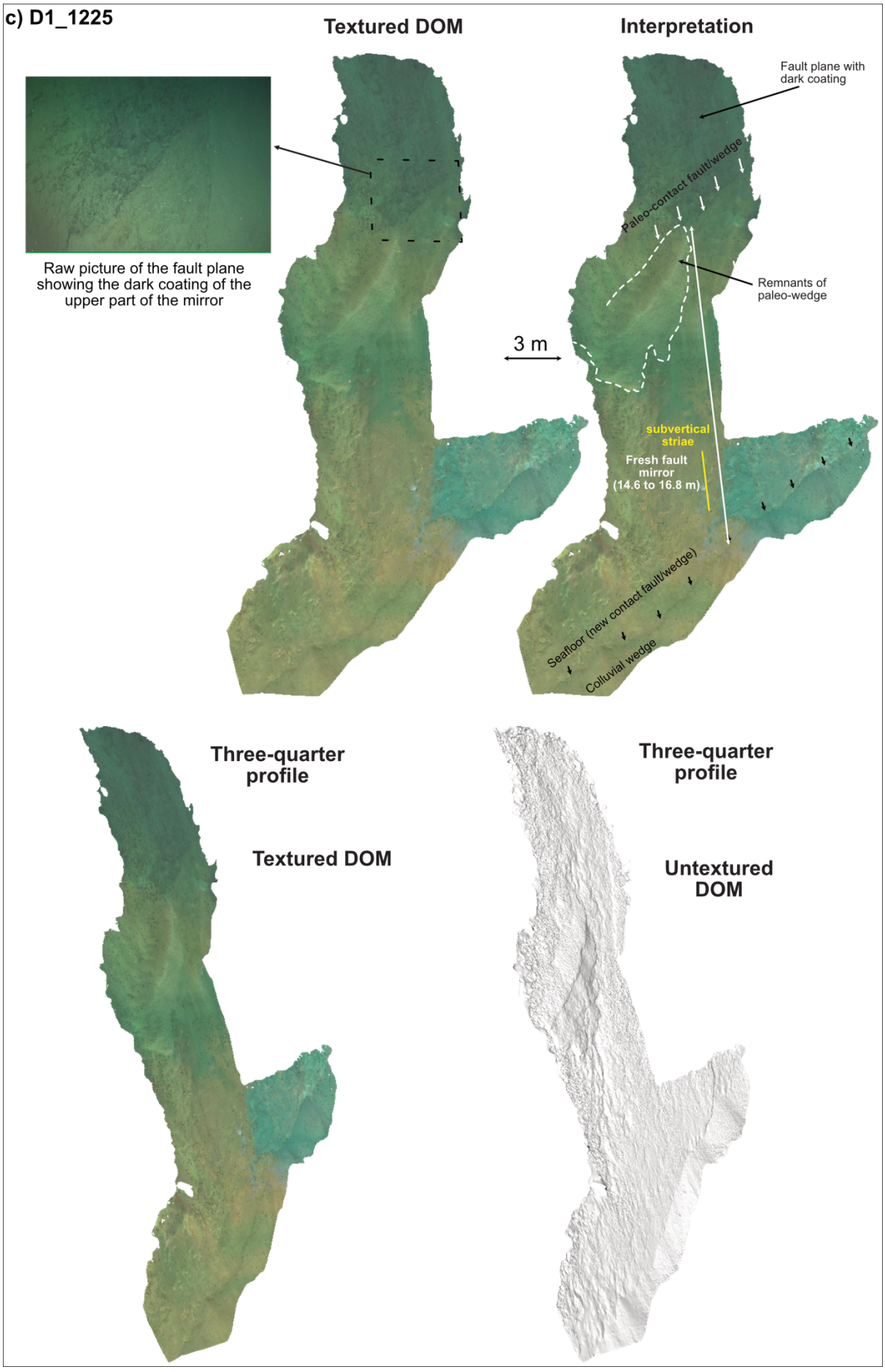
c) D1_1225
Textured DOM
Interpretation
Raw picture of the fault plane showing the dark coating of the upper part of the mirror
Fault plane with dark coating
Paleo-contact fault/wedge
Remnants of paleo-wedge
3 m
subvertical striae
Fresh fault mirror (14.6 to 16.8 m)
Seafloor (new contact fault/wedge)
Colluvial wedge
Three-quarter profile
Textured DOM
Three-quarter profile
Untextured DOM

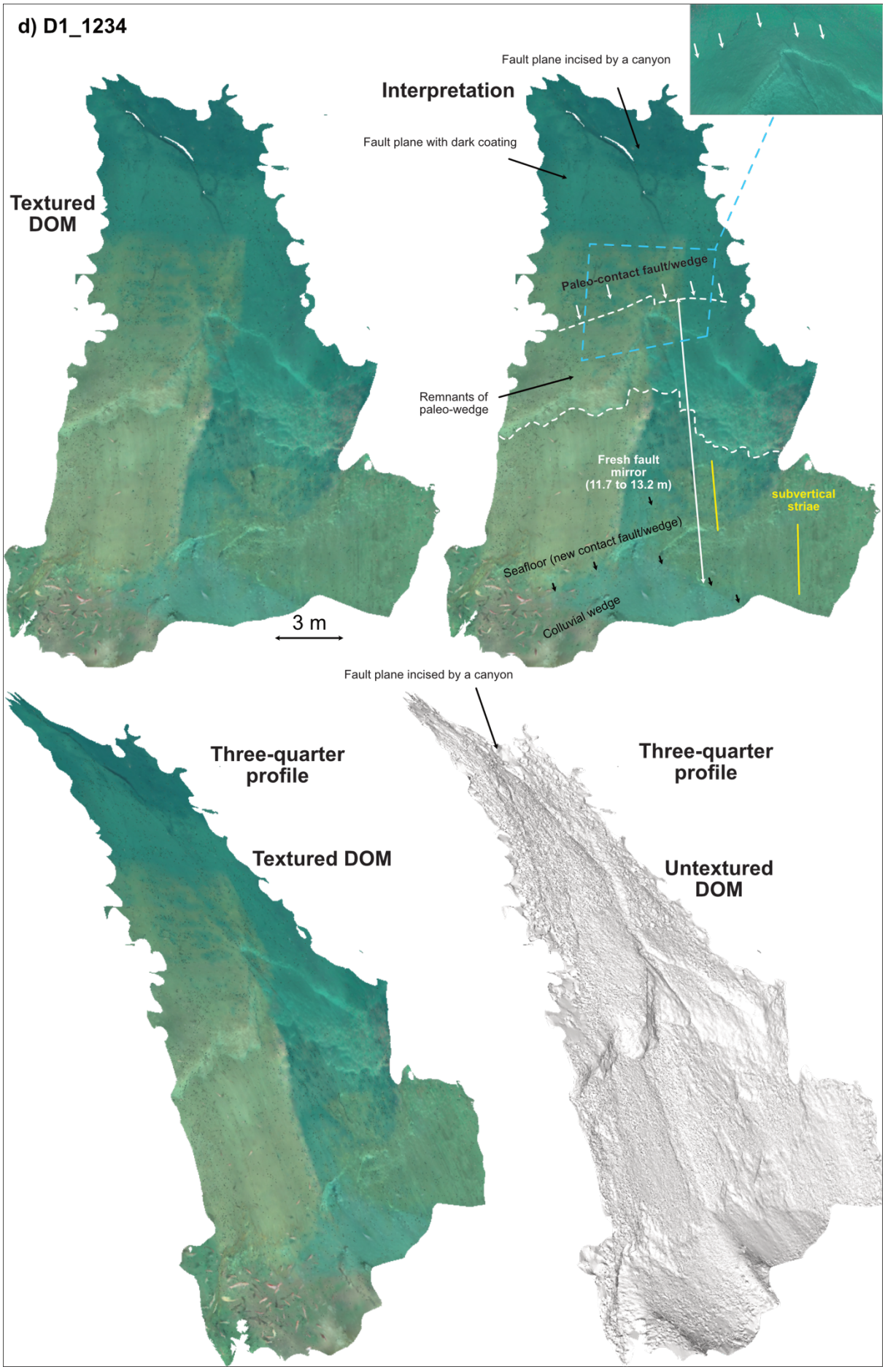
d) D1_1234
Fault plane incised by a canyon
Interpretation
Fault plane with dark coating
Textured DOM
Paleo-contact fault/wedge
Remnants of paleo-wedge
Fresh fault mirror (11.7 to 13.2 m)
subvertical striae
Seafloor (new contact fault/wedge)
Colluvial wedge
3 m
Fault plane incised by a canyon
Three-quarter profile
Textured DOM
Three-quarter profile
Untextured DOM

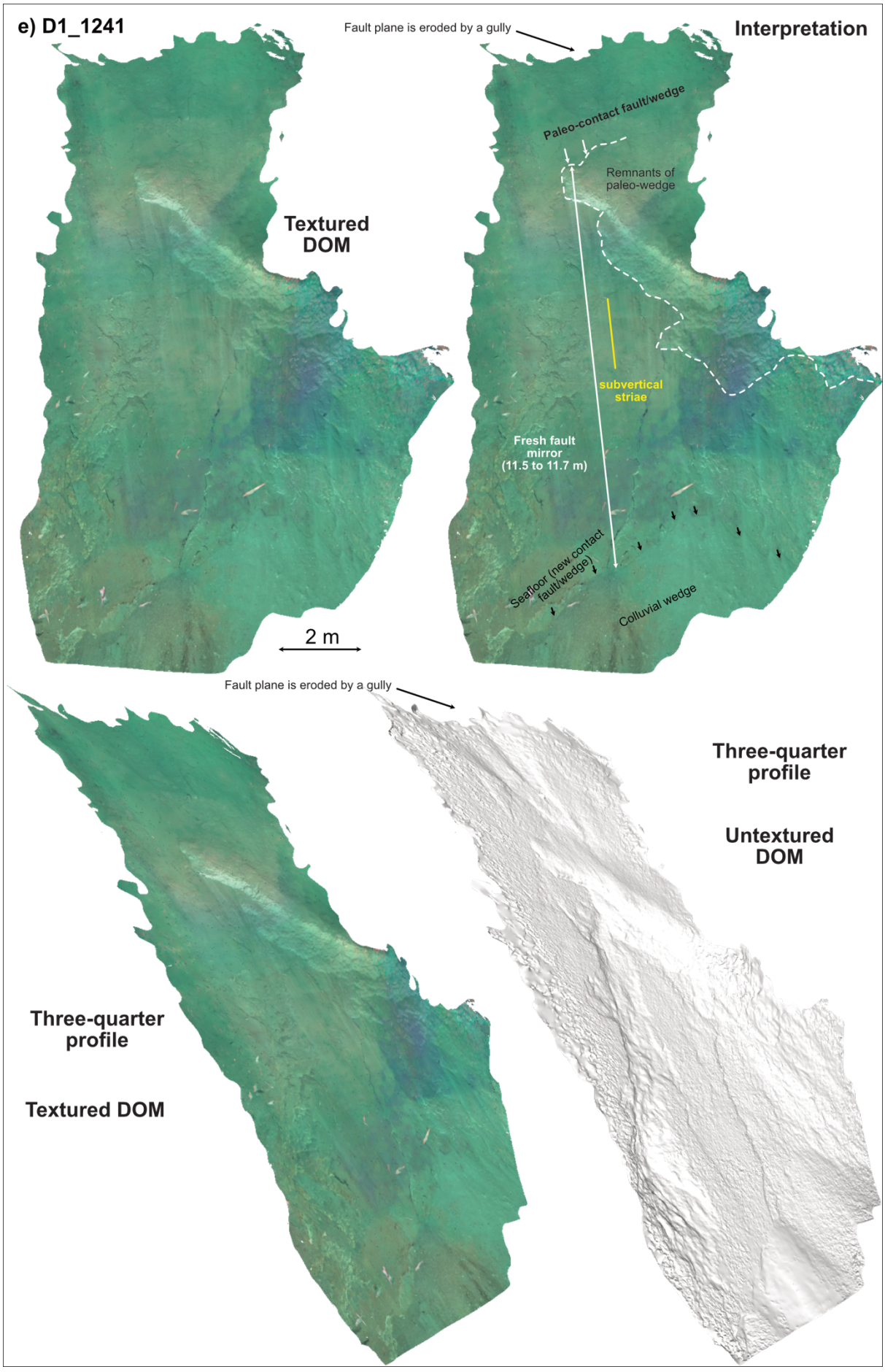
e) D1_1241
Fault plane is eroded by a gully
Interpretation
Textured DOM
Paleo-contact fault/wedge
Remnants of paleo-wedge
subvertical striae
Fresh fault mirror (11.5 to 11.7 m)
Seafloor (new contact fault/wedge)
Colluvial wedge
2 m
Fault plane is eroded by a gully
Three-quarter profile
Untextured DOM
Three-quarter profile
Textured DOM

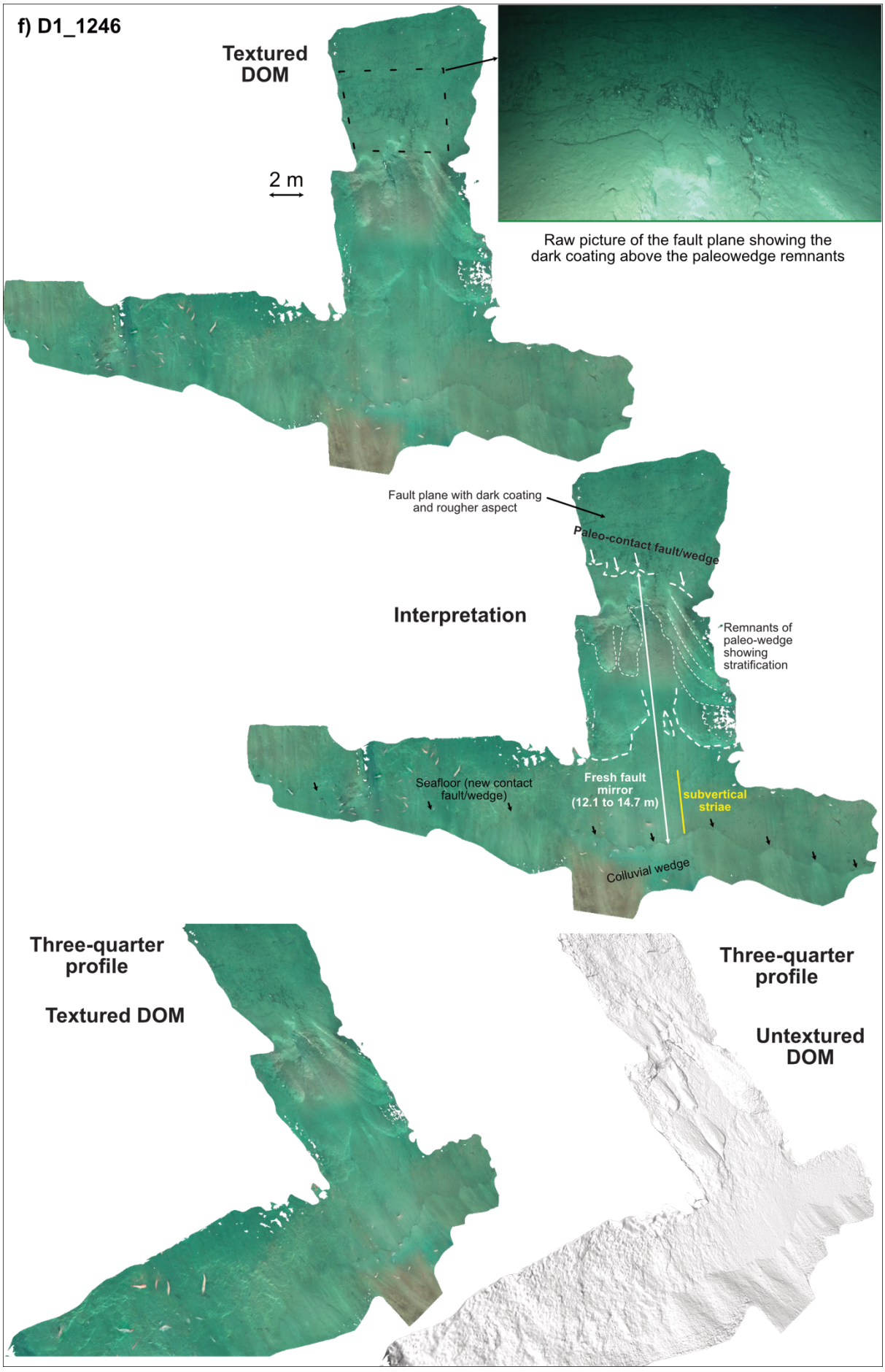
f) D1_1246
Textured DOM
2 m
Raw picture of the fault plane showing the dark coating above the paleowedge remnants
Fault plane with dark coating and rougher aspect
Paleo-contact fault/wedge
Interpretation
Remnants of paleo-wedge showing stratification
Seafloor (new contact fault/wedge)
Fresh fault mirror (12.1 to 14.7 m)
subvertical striae
Colluvial wedge
Three-quarter profile
Textured DOM
Three-quarter profile
Untextured DOM

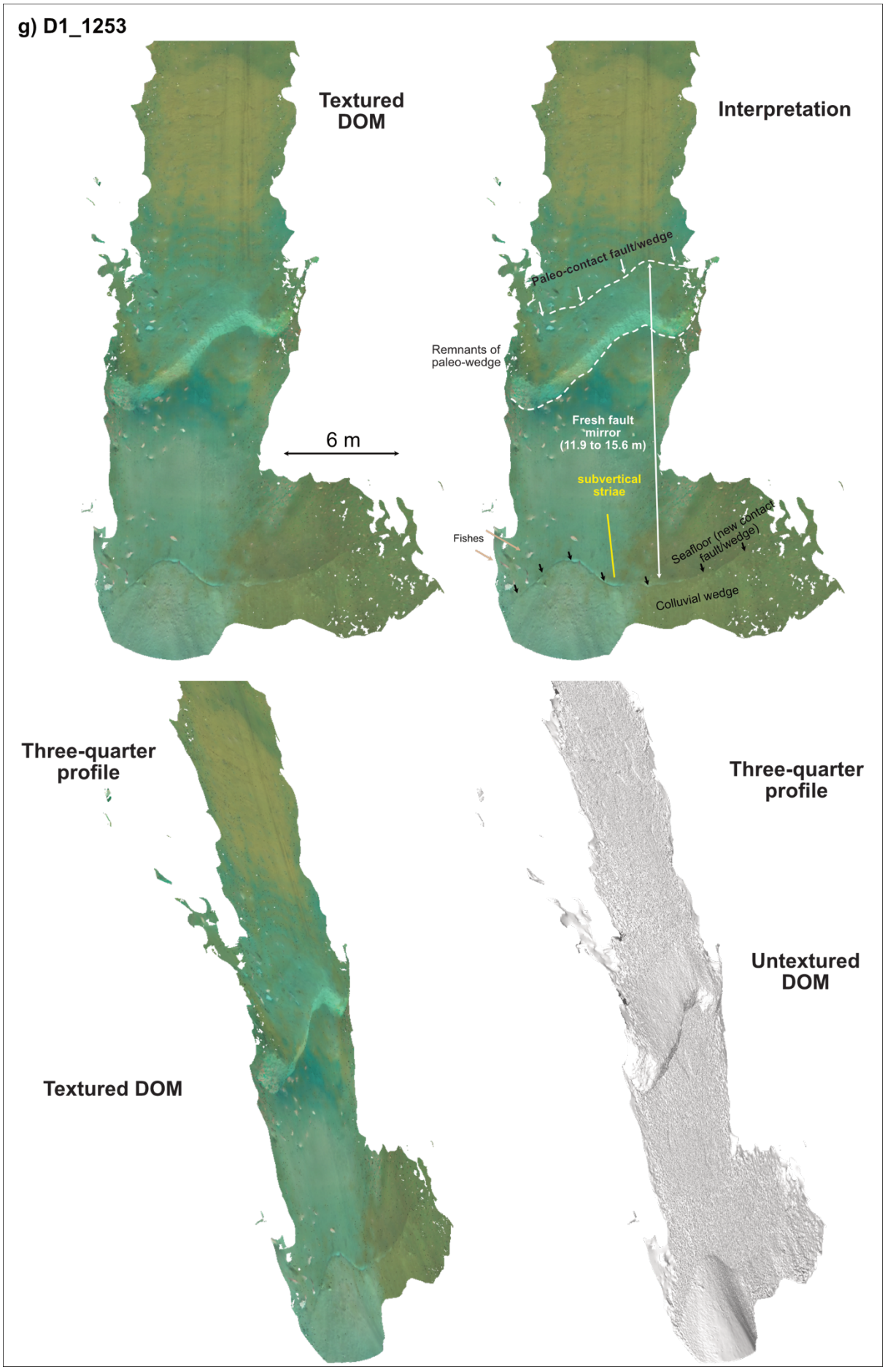
g) D1_1253
Textured DOM
Interpretation
Paleo-contact fault/wedge
Remnants of paleo-wedge
Fresh fault mirror (11.9 to 15.6 m)
subvertical striae
Fishes
Seafloor (new contact fault/wedge)
Colluvial wedge
6 m
Three-quarter profile
Three-quarter profile
Untextured DOM
Textured DOM

DOM name	Distance along strike (m)	Scarp Dip (°)			On-fault offset (m)			Vertical offset (m)			Horizontal extension (m)		
		Min	Mean	Max	Min	Mean	Max	Min	Mean	Max	Min	Mean	Max
D1_1116	0	40	50	60	10	11.75	13.5	6.4	9.0	11.7	5.0	7.6	10.3
D1_1136	100	50	55	60	**9.8**	10.5	11.2	7.5	8.6	9.7	4.9	6.0	7.2
D1_1225	235	49	51	53	14.6	15.7	**16.8**	11.0	12.2	13.4	8.8	9.9	11.0
D1_1234	270	40	45	50	11.7	12.45	13.2	7.5	8.8	10.1	7.5	8.8	10.1
D1_1241	295	35	40	45	11.5	11.6	11.7	6.6	7.5	8.3	8.1	8.9	9.6
D1_1246	316	40	42	44	12.1	13.4	14.7	7.8	9.0	10.2	8.7	10.0	11.3
D1_1253	340	42	45	48	11.9	13.75	15.6	8.0	9.7	11.6	8.0	9.7	11.6
			Mean values (m)		**11.7**	**12.7**	**13.7**	**7.8**	**9.2**	**10.7**	**7.3**	**8.7**	**10.1**

Supplementary Table S4: Scarp dip (measured on the 1 m DEM) and on-fault offset measurements (calculated with Matisse 3D[1], method A) for each Digital Outcrop Model (DOM). Corresponding vertical offsets and horizontal extensions are calculated.

Methods		C [54] On-fault offset (m)				B On-fault offset (m)				A [53] On-fault offset (m)					
DOM name	Distance along strike (m)	Min	Mean	Max	RMSE	Min	Mean	Max	BA Mean Square Error	Min	Mean	Max	RMSE	Mean all (m)	stdev
D1_1116	0	9.7	11.2	12.7	0.64	10.7	11.8	12.8	0.75	10.0	11.8	13.5	0.67	11.6	0.3
D1_1136	100	7.2	7.8	8.3	0.63	9.4	10.1	10.7	0.74	**9.8**	10.3	10.7	0.63	9.4	1.4
D1_1225	235	15.6	15.8	16.0	0.59	15.5	16.0	16.4	0.69	14.6	15.7	**16.8**	0.61	15.8	0.1
D1_1234	270	11.5	12.1	12.6	0.64	10.3	11.1	11.8	0.69	11.7	12.5	13.2	0.59	11.9	0.7
D1_1241	295	9.5	9.7	9.9	0.55	11.9	12.1	12.2	0.69	11.5	11.6	11.7	0.60	11.1	1.2
D1_1246	316	12.1	13.1	14.0	0.61	13.9	15.5	17.0	0.71	12.1	13.4	14.7	0.53	14.0	1.3
D1_1253	340	9.9	11.4	12.9	0.56	11.7	13.6	15.4	0.75	11.9	13.8	15.6	0.61	12.9	1.3
MEAN			**11.6**				**12.8**				**12.7**			**12.4**	**0.7**

Supplementary Table S5: Comparisons of the on-fault offset measurements performed on the DOMs, calculated with different methods and algorithms: A corresponds to MATISSE 3D software[1], B to 3DF ZEPHYR software, and C to Istenic et al. 2019[2].

Supplementary References:

1-Arnaubec, A., Ferrera, M., Escartín, J., Matabos, M., Gracias, N. and Opderbecke, J., 2023. Underwater 3D Reconstruction from Video or Still Imagery: Matisse and 3DMetrics Processing and Exploitation Software. *Journal of Marine Science and Engineering*, *11*(5), p.985.

2- Istenič, K.; Gracias, N.; Arnaubec, A.; Escartín, J.; Garcia, R. Scale Accuracy Evaluation of Image-Based 3D Reconstruction Strategies Using Laser Photogrammetry. Remote Sens. 2019, 11, 2093. https://doi.org/10.3390/rs11182093